WARSAW UNIVERSITY OF TECHNOLOGY Index 351733

FACULTY OF CIVIL ENGINEERING
COMMITTEE FOR CIVIL AND WATER ENGINEERING

POLISH ACADEMY OF SCIENCES ISSN 1230-2945

DOI: 10.24425/ace.2026.1330

ARCHIVES OF CIVIL ENGINEERING

Vol. LXXII ISSUE 3 2026

pp. 5 –21

Research paper

Forecasting demand for emergency relief materials resulting from flooding

Pengfei Gu[1], Yufeng Tian[2], Gaoxu Wang[3], Lang Wu[4], Miaomiao Li[5], Shuai Yang[6], Yekun Bai[7]

Abstract: Floods are among the most frequent and destructive natural disasters, causing substantial economic losses and casualties while posing challenges to emergency response in civil and disaster mitigation engineering. However, flood-related data often exhibit characteristics of "small sample size and insufficient information", limiting the effectiveness of traditional forecasting methods. This study proposes an improved GM$(1, 1)$ model based on grey system theory for dynamically predicting affected populations, integrated with inventory management to estimate emergency material demand. The model is validated using the June 2024 flood in Jiangxi Province, China. Results showed that: (1) The improved GM$(1, 1)$ model demonstrated high prediction accuracy, with the precision test Mean squared Error Ratio (MSER, $c = 0.27$) and Small Error Probability (SEP, $p = 1$) both meeting Grade I standards, making it suitable for forecasting affected populations; (2) Case analysis showed that the improved GM$(1, 1)$ model outperformed the traditional GM$(1, 1)$ model in terms of MSER ($c = 0.22 < 0.31$) and SEP ($p = 1.0 > 0.92$), with predicted values closer to actual values; (3) The dynamic demand model estimated material requirements from June 24 to July 6, including 15.48 million liters of drinking water, 14,700 tons of food, 8,700 tons of medicine, 2.9 million tents, 10.95 million quilts, and 29,000 signal stations. This study improves dynamic flood response by enabling emergency relief demand prediction and supporting deployments in civil engineering and disaster prevention, including resettlement planning, levee inspections, and identification of key transport nodes.

Keywords: flood disasters, improved GM(1,1) model, emergency relief materials, dynamic demand forecasting

[1]PhD., School of Civil Engineering, Jiangxi Science and Technology Normal University, Nanchang 330013, China, e-mail: gupengfei2020@163.com, ORCID: 0000-0002-2147-8690

[2]PhD., School of Civil Engineering, Jiangxi Science and Technology Normal University, Nanchang 330013, China, e-mail: wulang19812005@126.com, ORCID: 0009-0008-9255-7397

[3]MSc., School of Civil Engineering, Jiangxi Science and Technology Normal University, Nanchang 330013, China, e-mail: gxwang@nhri.cn, ORCID: 0000-0001-8878-0491

[4]MSc., School of Civil Engineering, Jiangxi Science and Technology Normal University, Nanchang 330013, China, e-mail: wulang19812005@126.com, ORCID: 0009-0008-3233-8985

[5]PhD., State Key Laboratory of Hydrology, Water Resources and Hydraulic Engineering, Nanjing Hydraulic Research Institute, Nanjing 210029, China, e-mail: 2826345769@qq.com, ORCID: 0009-0001-2796-9853

[6]PhD., School of Civil Engineering, Jiangxi Science and Technology Normal University, Nanchang 330013, China, e-mail: 1366210078@qq.com, ORCID: 0009-0007-6339-9257

[7]BSc., School of Civil Engineering, Jiangxi Science and Technology Normal University, Nanchang 330013, China, e-mail: 19047798100@163.com, ORCID: 0009-0008-7521-9978

1. Introduction

Flood disasters are among the most devastating natural hazards worldwide, causing significant economic losses and human casualties [1,2], and have long drawn global attention. In some countries, flood control has prompted policies such as floodplain development restrictions. While these measures reduce disaster risks, they have also raised concerns about constraints on regional development [3]. With ongoing climate change and urban expansion, extreme rainfall events are increasing. In 2020, floods in China affected 63.46 million people and caused direct economic losses of CNY 178.96 billion [4]. Against this backdrop, accurately forecasting emergency material demand and improving allocation efficiency has become an urgent challenge [5].

However, the sudden onset, dynamic evolution, widespread impact, and destructive nature of flood disasters result in data that are characterized by small samples and insufficient information, which severely limits rapid and accurate forecasting of material demand and hinders emergency engineering response [6,7]. Existing forecasting methods – such as case-based reasoning [8,9], fuzzy rough set theory [10,11], and back-propagation (BP) neural networks [12,13] – often rely on large-scale training data and involve high model complexity, making them unsuitable for flood scenarios with limited data and urgent response requirements.

Grey system theory provides an effective approach to addressing uncertainty under small-sample and poor-information conditions by revealing system trends through accumulated data sequences [14–16]. The GM(1,1) model, known for its simplicity and predictive capability, has been widely applied in various forecasting domains [17,18]. For example, Zhichao M et al. [19] integrated GM(1,1) with a material demand model for epidemic response, combining it with bi-objective optimization to improve allocation fairness. Research on GM(1,1) has explored improvements such as probabilistic accumulation [20] and seasonal adjustment [21], achieving enhanced accuracy. However, its application to flood-related emergency material demand remains limited due to the need for dynamic adaptability and higher precision to support emergency engineering operations.

This study proposes an improved GM(1,1) dynamic prediction model based on grey system theory to forecast the affected population during floods. Combined with inventory management theory, a population-based dynamic emergency material demand model is constructed to enhance forecasting accuracy. Using the June 2024 flood in Jiangxi Province, China as a case study, the model's effectiveness is validated. The results provide scientific and technical support for flood emergency response and engineering deployment.

2. Dynamic prediction model for flood-affected population

2.1. Development of the GM(1,1) forecasting model

Let $X^{(0)} = (x^{(0)}(1), x^{(0)}(2), \dots, x^{(0)}(t))$ represent the original sequence of affected population numbers, where $x^{(0)}(t)$ denotes the affected population at time t in the disaster area. The sequence $X^{(1)} = (x^{(1)}(1), x^{(1)}(2), \dots, x^{(1)}(t))$ is the first-order accumulated generating operation (1-AGO) of $X^{(0)}$, expressed as:

$$x^{(1)}(k) = \sum_{i=1}^{k} x^{(0)}(i), \quad k = 1, 2, \ldots, t \tag{2.1}$$

$Z^{(1)} = (z^{(1)}(2), z^{(1)}(3), \ldots, z^{(1)}(t))$ is the adjacent mean generating sequence of $X^{(1)}$, where:

$$z^{(1)}(k) = \frac{1}{2}\left(x^{(1)}(k) + x^{(1)}(k-1)\right), \quad k = 2, \ldots, t \tag{2.2}$$

The basic form of the GM$(1,1)$ forecasting model is:

$$x^{(0)}(k) + \lambda z^{(1)}(k) = \mu \tag{2.3}$$

Applying the least squares estimation to Eq. (2.3) [22], let:

$$\hat{a} = (\lambda, \mu)^T, \quad Y = \begin{bmatrix} x^{(0)}(2) \\ x^{(0)}(3) \\ \vdots \\ x^{(0)}(t) \end{bmatrix}, \quad B = \begin{bmatrix} -z^{(1)}(2) & 1 \\ -z^{(1)}(3) & 1 \\ \vdots & \vdots \\ -z^{(1)}(t) & 1 \end{bmatrix}.$$

Since $Y = B\hat{a}$, replacing $\mu - z^{(1)}(k)$ with $x^{(0)}(k)$ $(k = 2, 3, \ldots, t)$ yields the error sequence $\varepsilon = Y - B\hat{a}$. Let $\beta = \varepsilon^T \varepsilon = (Y - B\hat{a})^T (Y - B\hat{a})$, and when β reaches its minimum, the condition in Eq. (2.4) holds:

$$\begin{cases} \dfrac{\partial \beta}{\partial \lambda} = 2 \displaystyle\sum_{k=2}^{t} \left(x^{(0)}(k) + \lambda z^{(1)}(k) - \mu\right) z^{(1)}(k) = 0 \\ \dfrac{\partial \beta}{\partial \mu} = -2 \displaystyle\sum_{k=2}^{t} \left(x^{(0)}(k) + \lambda z^{(1)}(k) - \mu\right) = 0 \end{cases} \tag{2.4}$$

The solution is expressed as:

$$\begin{cases} \lambda = \dfrac{\dfrac{1}{t-1} \displaystyle\sum_{k=2}^{t} x^{(0)}(k) \sum_{k=2}^{t} z^{(1)}(k) - \sum_{k=2}^{t} x^{(0)}(k) z^{(1)}(k)}{\displaystyle\sum_{k=2}^{t} \left(z^{(1)}(k)\right)^2 - \frac{1}{t-1}\left(\sum_{k=2}^{t} z^{(1)}(k)\right)^2} \\ \mu = \dfrac{1}{t-1}\left[\displaystyle\sum_{k=2}^{t} x^{(0)}(k) + \lambda \sum_{k=2}^{t} z^{(1)}(k)\right] \end{cases} \tag{2.5}$$

$$\text{Furthermore: } \hat{a} = (B^T B)^{-1} B^T Y \begin{bmatrix} \dfrac{\dfrac{1}{t-1}\sum_{k=2}^{t} x^{(0)}(k) \sum_{k=2}^{t} z^{(1)}(k) - \sum_{k=2}^{t} x^{(0)}(k) z^{(1)}(k)}{\sum_{k=2}^{t} \left(z^{(1)}(k)\right)^2 - \dfrac{1}{t-1}\left(\sum_{k=2}^{t} z^{(1)}(k)\right)^2} \\ \dfrac{1}{t-1}\left[\sum_{k=2}^{t} x^{(0)}(k) + \lambda \sum_{k=2}^{t} z^{(1)}(k)\right] \end{bmatrix}$$

That is $\hat{a} = (\lambda, \mu)^T$, and thus, the time response equation of $\frac{\mathrm{d}x^{(1)}}{\mathrm{d}t} + \lambda x^{(1)} = \mu$ derived for $x^{(0)}(k) + \lambda z^{(1)}(k) = \mu$ is:

$$\hat{x}^{(1)}(t+1) = \left(x^{(1)}(1) - \frac{\mu}{\lambda}\right) e^{-\lambda t} + \frac{\mu}{\lambda} \tag{2.6}$$

where: $x^{(1)}(1) = x^{(0)}(1)$.

The estimated value of the original data is:

$$\hat{x}^{(0)}(k+1) = \hat{x}^{(1)}(k+1) - \hat{x}^{(1)}(k) = (1 - e^{\lambda}) \left(x^{(0)}(1) - \frac{\mu}{\lambda}\right) e^{-\lambda k} \tag{2.7}$$

where: $k = 1, 2, \ldots, t$.

2.2. Development of the improved GM(1,1) prediction model

The $\mathrm{GM}(1,1)$ model relies on historical data for modeling, making it difficult to capture time-dependent disturbance effects, which leads to reduced prediction accuracy over longer time horizons. To better adapt to the dynamic changes of the system, the original data sequence in the $\mathrm{GM}(1,1)$ prediction model is subjected to dimension-equivalent processing: the earliest data point $x^{(0)}(1)$ is removed, the most recent data point $x^{(0)}(t+1)$ is added, and a new data sequence $X^{(0)} = (x^{(0)}(2), x^{(0)}(3), \ldots, x^{(0)}(t+1))$ is generated. Using this new sequence as the original series, the basic form of the improved $\mathrm{GM}(1,1)$ prediction model can be expressed as follows:

$$x^{(0)}(k) + \lambda z^{(1)}(k) = \mu$$

where:

$$Y = \begin{bmatrix} x^{(0)}(3) \\ x^{(0)}(4) \\ \vdots \\ x^{(0)}(t+1) \end{bmatrix}, \quad B = \begin{bmatrix} -z^{(1)}(3) & 1 \\ -z^{(1)}(4) & 1 \\ \vdots & \vdots \\ -z^{(1)}(t+1) & 1 \end{bmatrix}$$

By substituting the updated data series into the least squares structure defined in Eqs. (2.4)–(2.7) and applying dimension-consistent processing, early data are progressively eliminated and new data are incorporated to construct a dynamically updated $\mathrm{GM}(1,1)$ prediction model. This approach assimilates the latest system state information while excluding outdated data interference. Based on the grey plane theory, it effectively narrows the prediction range, thereby enhancing both the model's accuracy and its adaptability to real-world conditions.

2.3. Validation of the prediction model's effectiveness

The effectiveness of the prediction model is evaluated using the Mean Squared Error Ratio (MSER) and the Small Error Probability (SEP). In this accuracy assessment, a smaller MSER and a larger SEP indicate better predictive performance. The evaluation process is as follows:

From the original data series $X^{(0)}$ and its estimated data series $\hat{X}^{(0)}$, the residual series $\varepsilon^{(0)}$ can be obtained as:

$$\varepsilon^{(0)} = \left(\varepsilon^{(0)}(1), \varepsilon^{(0)}(2), \ldots, \varepsilon^{(0)}(t)\right) \tag{2.8}$$

$$\varepsilon^{(0)}(k) = x^{(0)}(k) - \hat{x}^{(0)}(k), \quad k = 1, 2, \ldots, t \tag{2.9}$$

The variances of the original data series and the residual series are, respectively, calculated as:

$$s_1^2 = \frac{1}{t}\sum_{k=1}^{t}\left[x^{(0)}(k) - \overline{x}\right]^2 \tag{2.10}$$

$$s_2^2 = \frac{1}{t}\sum_{k=1}^{t}\left[\varepsilon^{(0)}(k) - \overline{\varepsilon}\right]^2 \tag{2.11}$$

where the respective means are:

$$\begin{cases} \overline{x} = \dfrac{1}{t}\displaystyle\sum_{k=1}^{t} x^{(0)}(k) \\ \overline{\varepsilon} = \dfrac{1}{t}\displaystyle\sum_{k=1}^{t} \varepsilon^{(0)}(k) \end{cases} \tag{2.12}$$

Thus, the test formula for the MSER c is given as:

$$c = \frac{s_2}{s_1} \tag{2.13}$$

The SEP p is defined as:

$$p = P\left\{\left|\varepsilon^{(0)}(k) - \overline{\varepsilon}\right| < 0.6745 s_1\right\} \tag{2.14}$$

The accuracy levels of the prediction model are shown in Table 1. Only by passing the validity test can the prediction results be considered reasonable and reliable. As shown in Table 1, a Level 1 prediction accuracy indicates the highest model precision and the strongest reliability of the prediction results.

Table 1. Model prediction accuracy grade

Accuracy grade	p	c
Level 1 (Excellent)	$0.95 \le p$	$c \le 0.35$
Level 2 (Qualified)	$0.80 \le p < 0.95$	$0.35 < c \le 0.50$
Level 3 (Barely)	$0.70 \le p < 0.80$	$0.50 < c \le 0.65$
Level 4 (Unqualified)	$p < 0.70$	$0.65 < c$

3. Development of a dynamic demand prediction model for emergency supplies in flood disasters

Emergency material demand is closely related to the scale and structure of the affected population, and this relationship becomes particularly evident when floods are triggered by the combined effects of heavy rainfall and upstream inflow. Population characteristics – such as total number, age, gender, and household structure – directly determine the types and quantities of supplies needed, including food, medicine, and tents.

3.1. Development of a dynamic demand prediction model for emergency supplies

Emergency materials are categorized into three types: daily consumables (e.g., drinking water, food), non-daily consumables (e.g., quilts, tents), and communication support equipment (e.g., signal base stations). The demand for all three types varies dynamically with the affected population under rainfall-driven flood conditions. Based on the affected population predicted by the improved GM$(1, 1)$ model, a dynamic emergency material demand model is developed by integrating category-specific demand functions and inventory management theory [23]. To account for the adequacy of supplies under emergency scenarios, safety stock levels are set, and service level and stockout rate parameters are introduced, forming the model described in Eqs. (3.1)–(3.3).

$$Q^i(t) = q_i \times \hat{x}(t) \times \Delta L + Z_{1-\alpha} \times D^i_Q(t) \times \Delta L, \quad i \in \{\text{Drinking water, food, medicine, and other essentials}\} \tag{3.1}$$

$$D^i_Q(t) = \sqrt{\frac{\sum_{k=0}^{t-1} \left[Q^i(t-k) - E^i(t)\right]^2}{t}} \tag{3.2}$$

$$E^i(t) = \frac{\sum_{k=0}^{t-1} Q^i(t-k)}{t} \tag{3.3}$$

where: i represents various emergency relief materials, such as drinking water, tents, etc.; $Q^i(t)$ denotes the demand for emergency material i in the disaster-stricken area at time t; q_i represents the per capita demand for emergency material i at time t; $\hat{x}(t)$ indicates the number of affected individuals in the disaster-stricken area; ΔL represents the time interval between two emergency material deliveries; $Z_{1-\alpha}$ corresponds to the service level coefficient determined by the stockout rate α of emergency materials; $D^i_Q(t)$ denotes the standard deviation (or variance measure) in demand for emergency material i at time t; $E^i(t)$ represents the predicted mean demand for material i at time t as it changes over time.

3.2. The impact of affected population age structure on emergency supply demand

Emergency material demand is influenced by the age structure of the affected population. The first category, including essential daily consumables such as drinking water and food, is particularly sensitive to physiological differences across age groups. For instance, water requirements vary significantly by age. According to the Public Health Emergency Research Center [24] and the Dietary Guidelines for Chinese Residents (2022) [25], the average daily water requirement is approximately 1200 mL per person. Children aged 2–5 require 600–800 mL/day, those aged 6–18 need 800–1400 mL/day, adult females require around 1500 mL/day, and adult males approximately 1700 mL/day, with adjustments depending on individual and climatic factors.

To estimate drinking water demand, four typical age structures are defined: A – rural households with mainly elderly and children (0–10); B – boarding groups dominated by adolescents (11–17); C – labor groups with adults (18+); D – mixed groups with balanced age distribution. Daily water demand is set at 1600 mL for adults (19–65) and 1200 mL for elderly (65+), using the upper limit of each age range for calculation.

$$W = \omega_1 \times 0.8 \times \hat{x}(t) \times \gamma + \omega_2 \times 1.4 \times \hat{x}(t) \times \gamma + \omega_3 \times 1.6 \times \hat{x}(t) \times \gamma + \omega_4 \times 1.2 \times \hat{x}(t) \times \gamma \tag{3.4}$$

where: W represents the daily drinking water demand in the disaster-affected area; ω_1, ω_2, ω_3, and ω_4 denote the proportions of children aged 2–5, children aged 6–18, adults aged 19–65, and elderly individuals over 65 years old among the affected population, respectively; γ is the seasonal coefficient, reflecting the impact of seasonal factors on drinking water demand.

Under normal conditions, the seasonal coefficient for drinking water is $\gamma = 1$, while during summer, the coefficient can be adjusted to γ with a value of 1.2 [26].

3.3. The impact of affected population family structures on emergency material demand

Non-daily consumables, such as tents and quilts, are typically distributed based on household units, and their demand is influenced by family structure. Taking tents as an example, common emergency relief tents are classified into two types based on area: 8 m^2 and 12 m^2 [27]. Assuming the tent area required per person is 2 m^2, three typical household structures are considered: (1) three-person household (2 adults + 1 child); (2) four-person household (2 elderly + 2 children); and (3) five-person household (2 elderly + 2 adults + 1 child).

For disaster-affected populations not grouped by household structure (e.g., types B and D), tent demand is calculated on a per capita basis of 2 m^2, resulting in a total tent area of $2\hat{x}(t)$. Accordingly, the demand forecasting formulas for 8 m^2 and 12 m^2 tents are defined as follows:

$$\begin{cases} T_1 = r_1 \times \hat{x}(t) \div 3 + r_2 \times \hat{x}(t) \div 4 \\ T_2 = r_3 \times \hat{x}(t) \div 5 \\ T = T_1 + T_2 \end{cases} \tag{3.5}$$

where: T represents the total tent demand; T_1 denotes the specific demand for 8 m^2 tents; T_2 indicates the demand for 12 m^2 tents; r_1, r_2, r_3 represent the proportions of three-person, four-person, and five-person households within the disaster-affected population, respectively.

3.4. The impact of affected population distribution on emergency material demand

Communication-related materials, such as signal base stations and satellite phones, cannot be allocated on a per-person basis. Their demand is significantly influenced by population density and distribution. Higher population density increases the coverage load, thereby requiring more equipment [28]. For example, the Huawei eNodeB 218 portable base station has a coverage radius of approximately 5 km and supports up to 400 users.

Considering population density differences, the equipment configuration standard is set at 1 unit per 400 people in high-density areas and 1 unit per 200 people in low-density areas. The communication equipment demand forecasting model is defined as follows:

$$C = f_1 \times \hat{x}(t) \div 400 + f_2 \times \hat{x}(t) \div 200 \tag{3.6}$$

where: C represents the demand for signal base stations; f_1 and f_2 denote the proportions of the affected population in densely distributed and sparsely distributed areas, respectively.

4. Case study analysis

The Poyang Lake region and its surrounding areas (Fig. 1) are low-lying, with poor drainage due to the confluence of rivers and lakes, and have historically experienced frequent flooding, with an average recurrence interval of 2.7 years since the 20th century [29–31]. In June 2024, Jiangxi Province recorded a 1.2°C decrease in average temperature and a 31% increase in precipitation compared to the historical average. Multiple stations exceeded warning water levels (e.g., Hukou Station exceeded by 1.97 m [32]), and the Xiu River basin experienced a once-in-a-century flood event [33]. Precipitation maps derived from the GEE remote sensing platform (Fig. 2) show that northern parts of the basin experienced multiple rounds of heavy rainfall from June 21 to 27, with daily totals generally exceeding 1.2×10^8 m^3. Notably, rainfall intensified on June 24–25 and closely matched the temporal and spatial distribution of the disaster, indicating that accumulated rainfall was a key contributing factor. This study takes the flood event from June 23 to July 6 in the Poyang Lake basin as a case. First, an improved GM$(1,1)$ model is developed to predict the affected population. Then, an emergency supply demand model is constructed based on population structure. Finally, the demand for key supplies such as drinking water, food, tents, and communication stations is quantified, and the results are discussed in the context of decision support for civil and disaster mitigation engineering deployment.

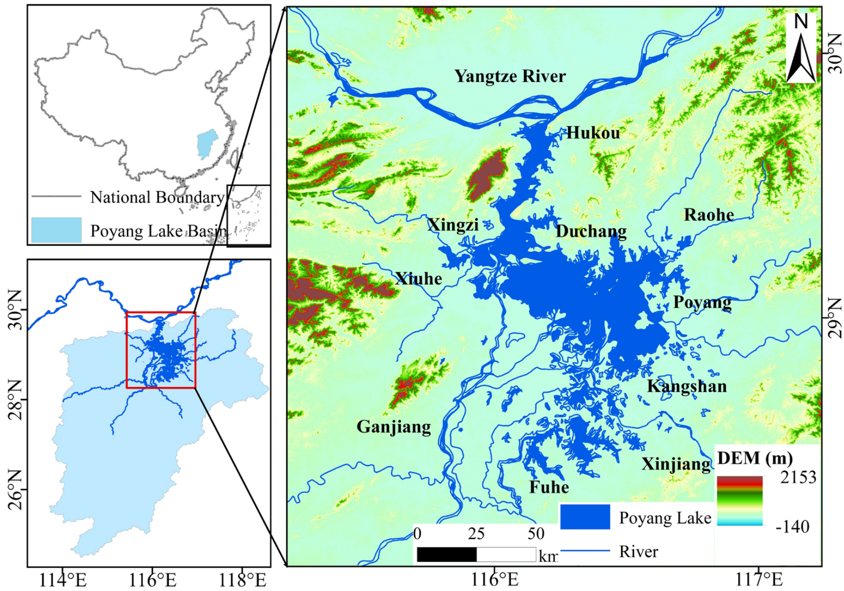

Fig. 1. Study area

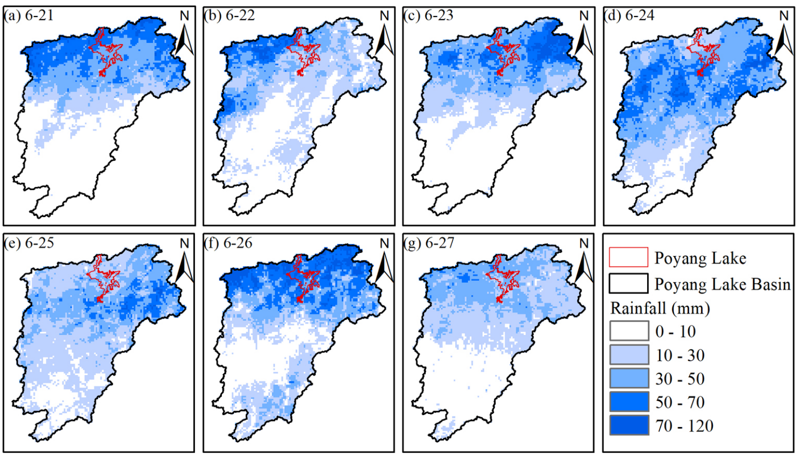

Fig. 2. Precipitation maps derived from the GEE remote sensing platform

4.1. Data preprocessing

Based on the statistics of affected population released by the Jiangxi Provincial Flood Control and Drought Relief Headquarters from June 23 to June 27, the initial sequence of affected population data (with one day as one time period, unit: 10,000 people) is organized as follows:

$$X^{(0)} = (0.12, 6.12, 24.62, 36.32, 44.12, 51.92, 56.72, 60.12, 67.42, 71.32, 76.92, 80.12, 84.22, 86.22)$$

Selecting the first five data points from the above sequence as the initial data for modeling yields the following: $X^{(0)} = (0.12, 6.12, 24.62, 36.32, 44.12)$.

The first-order cumulative sequence $X^{(1)}$ of $X^{(0)}$ is expressed as:

$X^{(1)} = (0.12, 6.24, 30.86, 67.18, 111.30)$ the neighboring mean generation sequence $Z^{(1)}$ of $X^{(1)}$ is defined as: $Z^{(1)} = (3.18, 18.55, 49.02, 89.24, 137.26)$.

$$\text{Get:}\quad Y = \begin{bmatrix} 6.12 \\ 24.62 \\ 36.32 \\ 44.12 \end{bmatrix}, \quad B = \begin{bmatrix} -3.18 & 1 \\ -18.55 & 1 \\ -49.02 & 1 \\ -89.24 & 1 \end{bmatrix}, \quad \hat{a} = (B^T B)^{-1} B^T Y = \begin{bmatrix} \lambda \\ \mu \end{bmatrix} = \begin{bmatrix} -0.40 \\ 11.63 \end{bmatrix}$$

Substituting into Eq. (2.6), the time response equation for $X^{(1)}$ is obtained as:

$$\begin{cases} \hat{x}^{(1)}(t+1) = 28.89e^{-0.40t} - 28.77 \\ \hat{x}^{(0)}(t+1) = \hat{x}^{(1)}(t+1) - \hat{x}^{(1)}(t) \end{cases} \tag{4.1}$$

4.2. Precision testing of simulated values

Using the methods of MSER and SEP described in Section 2.3, the predictive model is validated for effectiveness. By substituting $t = 1, 2, 3, 4$ into Eq. (4.1), the simulated value sequence is obtained as: $(\hat{x}^{(0)}(2), \hat{x}^{(0)}(3), \hat{x}^{(0)}(4), \hat{x}^{(0)}(5)) = (14.39, 21.56, 32.29, 48.38)$ the residual sequence $\varepsilon^{(0)}$ can be obtained as:

$$\varepsilon^{(0)} = (\varepsilon^{(0)}(2), \varepsilon^{(0)}(3), \varepsilon^{(0)}(4), \varepsilon^{(0)}(5)) = (-8.27, 3.06, 4.03, -4.26)$$

Thus, the mean of the original data sequence is $\overline{x} = 22.26$, and its variance is $s_1^2 = 286.36$. The mean of the residual sequence is $\overline{\varepsilon} = -1.09$, and its variance is $s_2^2 = 21.24$. Consequently: MSER: $c = s_1/s_2 = 0.27$; SEP: $p = 1$.

By comparing the results in Table 1: $c = 0.27 \leq 0.35$ (Grade 1: Excellent); $p = 1 \geq 0.95$ (Grade 1: Excellent).

Both the MSER and the SEP accuracy tests achieve Grade 1 (Excellent). Therefore, the model is validated as suitable for predicting the affected population in disaster scenarios.

4.3. Prediction of the affected population

According to the construction process of the improved GM$(1, 1)$ model, a sliding window approach is applied to perform 10 rounds of dynamic prediction using data from June 23 to July 6. In each round, the oldest data point is replaced by the latest available one. The initial simulation is based on data from June 23 to 27, with the original sequence updated sequentially thereafter. A total of ten simulation results are obtained and evaluated for accuracy, as detailed in Table 2.

As shown in Table 2, the accuracy values of the 10 prediction iterations all fall within the Grade 1 range, indicating that the improved GM$(1, 1)$ prediction model has successfully passed the validity test. The actual and predicted values of the affected population from June 27 to July 6 are presented in Table 3, and their comparison is illustrated in Fig. 3.

Table 2. Simulation value and prediction accuracy value of the number of people affected by the disaster

Calculation Times	Simulated Value (10,000 people)				p	c
1	14.39	21.56	32.29	48.38	1.0	0.27
2	22.22	33.99	42.43	52.98	1.0	0.11
3	37.57	43.37	50.06	57.79	1.0	0.10
4	45.68	50.36	55.51	61.19	1.0	0.14
5	51.69	56.29	61.29	66.73	1.0	0.08
6	56.41	61.11	66.20	71.71	1.0	0.11
7	61.04	66.01	71.39	77.20	1.0	0.10
8	67.52	71.62	75.97	80.58	1.0	0.07
9	71.99	75.93	80.10	84.50	1.0	0.01
10	77.14	80.20	83.40	86.70	1.0	0.08

Table 3. Actual and predicted number of people affected (10,000 people)

Date	6.27	6.28	6.29	6.30	7.1	7.2	7.3	7.4	7.5	7.6
Actual Value	44.12	51.92	56.72	60.12	67.42	71.32	76.92	80.12	84.22	86.22
Predicted Value	48.38	52.98	57.79	61.19	66.73	71.71	77.20	80.58	84.50	86.70

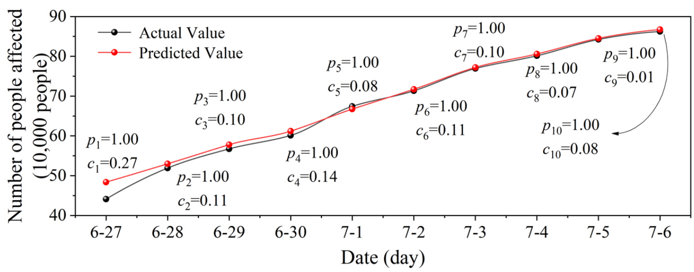

Fig. 3. Comparison between the actual and predicted numbers of people affected by the disaster

4.4. Comparing results of traditional and improved GM(1,1) prediction models

To demonstrate the superiority of the improved GM$(1,1)$ prediction model, a comparative analysis of the prediction results between the traditional and improved GM$(1,1)$ models was conducted. The initial sequence for the traditional GM$(1,1)$ prediction model was selected as: $X^{(0)} = (0.12, 6.12, 24.62, 36.32, 44.12, 51.92, 56.72, 60.12, 67.42, 71.32, 76.92, 80.12, 84.22)$ while the initial sequence for the improved GM$(1,1)$ prediction model was selected as: $X^{(0)} = (6.12, 24.62, 36.32, 44.12, 51.92, 56.72, 60.12, 67.42, 71.32, 76.92, 80.12, 84.22, 86.22)$ By performing calculations, the results $\hat{a} = \begin{bmatrix} \lambda \\ \mu \end{bmatrix} = \begin{bmatrix} -0.11 \\ 28.31 \end{bmatrix}$ for the traditional GM$(1,1)$ prediction model and $\hat{a} = \begin{bmatrix} \lambda \\ \mu \end{bmatrix} = \begin{bmatrix} -0.08 \\ 36.02 \end{bmatrix}$ for the improved GM$(1,1)$ prediction model were obtained. Substituting these results into Eq. (2.6), the time response equations for $X^{(1)}$ in the traditional and improved GM$(1,1)$ models are derived as G_1, G_2, respectively.

$$G_1 = \begin{cases} \hat{x}^{(1)}(t+1) = 257.36e^{-0.11t} - 257.48 \\ \hat{x}^{(0)}(t+1) = \hat{x}^{(1)}(t+1) - \hat{x}^{(1)}(t) \end{cases} \tag{4.2}$$

$$G_2 = \begin{cases} \hat{x}^{(1)}(t+1) = 450.25e^{-0.08t} - 450.37 \\ \hat{x}^{(0)}(t+1) = \hat{x}^{(1)}(t+1) - \hat{x}^{(1)}(t) \end{cases} \tag{4.3}$$

Eq. (4.2) represents the GM$(1,1)$ time response equation of $X^{(1)}$ in the traditional GM$(1,1)$ prediction model, while Eq. (4.3) represents the GM$(1,1)$ time response equation of $X^{(1)}$ in the improved GM$(1,1)$ prediction model.

By performing calculations based on Eq. (4.2) and Eq. (4.3), the prediction results of the traditional GM$(1,1)$ model and the improved GM$(1,1)$ model are obtained, as shown in Table 4. A comparison is illustrated in Fig. 4, which demonstrates that the improved GM$(1,1)$ model provides a better fit than the traditional GM$(1,1)$ model.

Table 4. Comparison of prediction results between traditional GM$(1,1)$ model and improved GM$(1,1)$ model (10,000 people)

Date	Actual Value	Traditional Model Prediction Value	Improved Model Prediction Value
June 23rd	0.12	0.12	–
June 24th	6.12	29.87	6.12
June 25th	24.62	33.18	38.07
June 26th	36.32	36.85	41.33
June 27th	44.12	40.94	44.87
June 28th	51.92	45.47	48.71
June 29th	56.72	50.51	52.88
June 30th	60.12	56.11	57.41
July 1st	67.42	62.33	62.33
July 2nd	71.32	69.23	67.66
July 3rd	76.92	76.91	73.46
July 4th	80.12	85.43	79.76
July 5th	84.22	94.89	86.58
July 6th	86.22	–	94.00

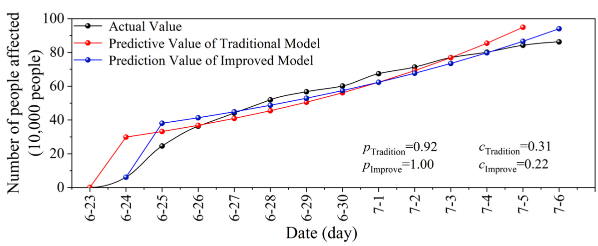

Fig. 4. Comparison of prediction results between traditional GM$(1,1)$ model and improved GM$(1,1)$ model

Through the validity testing of the GM$(1, 1)$ model using the SEP and MSER, as shown in Table 5, the results are as follows:

The SEP for the traditional GM$(1, 1)$ prediction model is 0.92, corresponding to a prediction accuracy grade of Level 2. In contrast, the improved GM$(1, 1)$ prediction model achieves a SEP of 1.0, corresponding to a prediction accuracy grade of Level 1. Additionally, the MSER for the traditional GM$(1, 1)$ model is 0.31, while that for the improved GM$(1, 1)$ model is 0.22. Both models achieve a prediction accuracy grade of Level 1 based on the MSER.

Overall, the improved GM$(1, 1)$ model demonstrates higher accuracy, and its prediction results are more closely aligned with the actual data.

Table 5. Values of each parameter

	Raw Data Mean $\overline{x}$	Residual Mean $\overline{\varepsilon}$	Raw Data Variance s_1^2	Residual Variance s_2^2	p	c
Traditional Model	50.77	−1.68	691.06	67.67	0.92	0.31
Improved Model	57.40	−0.54	546.47	27.12	1.00	0.22

The improved GM$(1, 1)$ prediction model incorporates dynamic data, allowing for the timely integration of new information. This approach aligns more closely with real-world development trends, significantly reducing the randomness of the data sequence and enhancing the stability and accuracy of the data. As a result, the improved GM$(1, 1)$ model achieves higher prediction accuracy.

4.5. Emergency relief material demand forecasting

Based on the disaster-affected population predicted by the improved GM$(1, 1)$ model and the structural characteristics of the affected groups, the emergency material demand for the Poyang Lake region and surrounding areas is estimated using Eqs. (3.1)–(3.3). The forecast covers drinking water, food, medicine, tents, quilts, and signal base stations.

Population structure data are derived from the National Bureau of Statistics [34] and Jiangxi Provincial Bureau of Statistics [35], indicating that the region is predominantly composed of elderly- and child-staying households. The proportions of the population aged 2–5, 6–18, 19–65, and over 65 are 36.21%, 18.16%, 21.80%, and 23.77%, respectively [36, 37]. The proportions of three-, four-, and five-person households are 33.34%, 41.57%, and 25.09% [34].

q_1 denotes the daily drinking water requirement per person, set as 800 mL, 1400 mL, 1600 mL, and 1200 mL for each age group, respectively. q_2 represents daily food demand per person, valued at 1.18 kg, 1.4 kg, 1.6 kg, and 1.3 kg for the respective age groups. $q_3 = 0.79$ indicates a per capita daily demand of 0.79 boxes of anti-inflammatory medicine. The interval between two consecutive supply deliveries is $\Delta L = 1$; the stockout rate is $\alpha = 0.05$, and the safety stock service level coefficient is $Z_{1-\alpha} = 1.65$ [38]. The proportion of disaster victims in densely versus sparsely populated areas is set as $f_1 = 0.94$, $f_2 = 0.06$. By substituting these parameter values into Eqs. (3.1)–(3.6), the demand for each type of material is calculated, with the results presented in Table 6.

Table 6. Predicted value of emergency relief material demand

Date	First Kind			Second Kind		Third Kind
	Drinking Water (L)	Food (t)	Medicines (t)	Tent (ten thousand tops)	Quilts (ten thousand)	Signal base stations (station)
6.24	86509.38	81.97	48.35	1.62	6.12	162
6.25	910733.89	862.91	508.98	17.10	64.43	1707
6.26	954730.84	904.59	533.58	17.91	67.54	1790
6.27	995188.82	942.93	556.18	18.67	70.40	1866
6.28	1044647.26	989.80	583.83	19.60	73.90	1958
6.29	1104789.91	1046.78	617.44	20.74	78.16	2071
6.30	1175989.03	1114.24	657.23	22.07	83.19	2205
7.1	1258483.62	1192.40	703.34	23.61	89.03	2359
7.2	1352366.04	1281.35	755.80	25.38	95.67	2535
7.3	1458432.77	1381.85	815.08	27.36	103.18	2734
7.4	1577058.42	1494.25	881.37	29.60	111.57	2957
7.5	1708452.65	1618.74	954.81	32.05	120.86	3203
7.6	1853838.13	1756.50	1036.06	34.78	131.15	3475
Total	15481220.76	14668.31	8652.05	290.49	1095.2	29022

4.6. Decision support for emergency engineering deployment based on model predictions

Model predictions indicate a rapid increase in the affected population and a significant rise in emergency supply demand in the Poyang Lake basin during June 23 to July 6, 2024. These results provide quantitative support for emergency resource planning and engineering deployment, particularly in road repair, shelter site selection, and levee inspection and reinforcement. As a key ecological and transportation hub in northern Jiangxi Province, the basin suffered severe impacts from heavy rainfall in late June, including a landslide in Xianqiao Village, Xiushui County, which disrupted transportation [39] (Fig. 5). At the same time, water levels at Hukou Station reached 19.52 m, with the Jiujiang section exceeding the warning level by approximately 1.0 m [40] (Fig. 6). Landslide disasters often require engineering interventions such as anti-slide piles and retaining walls [41], highlighting the need for early deployment of resources based on terrain characteristics. Based on the model outputs, key traffic restoration points and high-demand zones can be identified, enabling optimized allocation of repair resources and levee patrol strategies to reduce the risk of secondary disasters.

Fig. 5. Landslide site in Xianqiao Village, Lukou Township, Xiushui County, Jiujiang City, June 2024

Fig. 6. Real-time water levels at Jiujiang Station of the Yangtze River and water levels at Hukou Station of Poyang Lake, June 2024

5. Conclusions

(1) Accuracy of the Improved GM(1, 1) Model: The improved GM(1, 1) prediction model passed accuracy tests, achieving a MSER of $c = 0.27$ and a SEP of $p = 1.0$. Both tests yielded a grade of Level 1 (excellent), confirming its suitability for predicting affected populations.

(2) Compared with the traditional GM(1, 1) forecasting model, the improved GM(1, 1) model produces results that are closer to the actual values. The MSER ($c = 0.22$) and SEP ($p = 1.0$) of the improved model outperformed those of the traditional GM(1, 1) model ($c = 0.31$) and ($p = 0.92$), respectively.

(3) Based on the improved model prediction, the total emergency material demand from June 24 to July 6, 2024, is as follows: drinking water: 15.48 million liters; food: 14,700 tons; medicine: 8,700 tons; tents: 2.905 million units; quilts: 10.952 million units; signal base stations: 29,000 units.

References

[1] Y. Li, S. Ye, Q. Wu, Y. Wu, and S. Qian, "Analysis and countermeasures of the '7.20' flood in Zhengzhou", *Journal of Asian Architecture and Building Engineering*, vol. 22, no. 6, pp. 3782–3798, 2023, doi: 10.1080/13467581.2023.2208195.

[2] J. Li, J. Gao, N. Li, Y. Yao, and Y. Jiang, "Risk Assessment and Management Method of Urban Flood Disaster", *Water Resources Management*, vol. 37, no. 5, pp. 2001–2018, 2023, doi: 10.1007/s11269-023-03467-3.

[3] J. Sobieraj and D. Metelski, "Spatial planning policy towards floodplains and environmental protection as obstacles to the development of settlements on the Lower Bug", *Archives of Civil Engineering*, vol. 69, no. 2, pp. 583–605, 2023, doi: 10.24425/ace.2023.145286.

[4] "The State Council Information Office Holds a Press Conference on Flood Control and Disaster Relief Efforts", Press Office Website. [Online]. Available: https://www.gov.cn/xinwen/2020-08/13/content_5534534.htm (in Chinese).

[5] M. Rubinato, et al., "Urban and river flooding: Comparison of flood risk management approaches in the UK and China and an assessment of future knowledge needs", *Water Science and Engineering*, vol. 12, no. 4, pp. 274–283, 2019, doi: 10.1016/j.wse.2019.12.004.

[6] C. Li, et al., “Review on Urban Flood Risk Assessment”, *Sustainability*, vol. 15, no. 1, art. no. 765, 2022, doi: 10.3390/su15010765.

[7] W.L. Filho, et al., “Assessing the impacts of climate change in cities and their adaptive capacity: Towards transformative approaches to climate change adaptation and poverty reduction in urban areas in a set of developing countries”, *Science of The Total Environment*, vol. 692, pp. 1175–1190, 2019, doi: 10.1016/j.scitotenv.2019.07.227.

[8] L. Fei and Y. Wang, “Demand prediction of emergency materials using case-based reasoning extended by the Dempster-Shafer theory”, *Socio-Economic Planning Sciences*, vol. 84, art. no. 101386, 2022, doi: 10.1016/j.seps.2022.101386.

[9] J. Shao, C. Liang, Y. Liu, J. Xu, and S. Zhao, “Relief demand forecasting based on intuitionistic fuzzy case-based reasoning”, *Socio-Economic Planning Sciences*, vol. 74, art. no. 100932, 2020, doi: 10.1016/j.seps.2020.100932.

[10] W. Li and B. Yang, “Three-way decisions with fuzzy probabilistic covering-based rough sets and their applications in credit evaluation”, *Applied Soft Computing*, vol. 136, art. no. 110144, 2023, doi: 10.1016/j.asoc.2023.110144.

[11] B. Sun, W. Ma, and H. Zhao, “A fuzzy rough set approach to emergency material demand prediction over two universes”, *Applied Mathematical Modelling*, vol. 37, no. 10-11, pp. 7062–7070, 2013, doi: 10.1016/j.apm.2013.02.008.

[12] F. Chen, J. Chen, and J. Liu, “Forecast of flood disaster emergency material demand based on IACO-BP algorithm”, *Neural Computing and Applications*, vol. 34, no. 5, pp. 3537–3549, 2021, doi: 10.1007/s00521-021-05883-1.

[13] R. Mohammadi, S.M.T.F. Ghomi, and F. Zeinali, “A new hybrid evolutionary based RBF networks method for forecasting time series”, *Engineering Applications of Artificial Intelligence*, vol. 36, pp. 204-214, 2014, doi: 10.1016/j.engappai.2014.07.022.

[14] Y.-W. Wang, Z.-Z. Shen, and Y. Jiang, “Comparison of ARIMA and GM(1,1) models for prediction of hepatitis B in China”, *PLoS One*, vol. 13, no. 9, art. no. e0201987, 2018, doi: 10.1371/journal.pone.0201987.

[15] J. Deng, *Basic Methods of Grey Systems*. Wuhan: Huazhong University of Science and Technology Press, 2005 (in Chinese).

[16] S.F. Liu and J.L. Deng, “The Range Suitable for GM(1,1)”, *Systems Engineering Theory and Practice*, vol. 20, no. 5, pp. 121–124, 2000, doi: 10.12011/1000-6788(2000)5-121 (in Chinese).

[17] S. Guo, Y. Wen, X. Zhang, and H. Chen, “Runoff prediction of lower Yellow River based on CEEMDAN-LSSVM-GM(1,1) model”, *Scientific Reports*, vol. 13, art. no. 1511, 2023, doi: 10.1038/s41598-023-28662-5.

[18] Y.-C. Hu, “Forecasting tourism demand using fractional grey prediction models with Fourier series”, *Annals of Operations Research*, vol. 300, no. 2, pp. 467–491, 2021, doi: 10.1007/s10479-020-03670-0.

[19] Z. Ma, J. Zhang, and S. Gao, “Research on emergency material demand based on urgency and satisfaction under public health emergencies”, *PLoS One*, vol. 18, no. 3, art. no. e0282796, 2023, doi: 10.1371/journal.pone.0282796.

[20] K.D. Yin, K. Zhang, and W.D. Yang, “A discrete GM(1,1) model based on probabilistic accumulation and its application to offshore gas production forecasting”, *Systems Engineering Theory and Practice*, vol. 44, no. 8, pp. 2733–2746, 2024, doi: 10.12011/SETP2023-1876 (in Chinese).

[21] Z.-X. Wang, Q. Li, and L.-L. Pei, “A seasonal GM(1,1) model for forecasting the electricity consumption of the primary economic sectors”, *Energy*, vol. 154, pp. 522–534, 2018, doi: 10.1016/j.energy.2018.04.155.

[22] Y. Liu, R. Du, and D. Niu, “Forecast of Coal Demand in Shanxi Province Based on GA – LSSVM under Multiple Scenarios”, *Energies*, vol. 15, no. 17, art. no. 6475, 2022, doi: 10.3390/en15176475.

[23] E.E. Ozguven and K. Ozbay, “An RFID-based inventory management framework for emergency relief operations”, *Transportation Research Part C: Emerging Technologies*, vol. 57, pp. 166–187, 2015, doi: 10.1016/j.trc.2015.06.021.

[24] “Today, have you had a good drink?”, Public Health Emergency Consulting Center. [Online]. Available: https://eph.njmu.edu.cn/2024/0226/c9772a256292/page.htm (in Chinese).

[25] “Dietary Guidelines For Chinese Residents”, Chinese Nutrition Society. [Online]. Available: http://dg.cnsoc.org/ (in Chinese).

[26] L. Zhang, “Research on Dynamic Demand Prediction of Emergency Relief Materials Oriented to the Temporal and Spatial Change of Earthquake Disaster Losses”, *Disaster Science*, vol. 33, no. 3, pp. 161–164, 2018, doi: 10.3969/j.issn.1000-811X.2018.03.031 (in Chinese).

[27] Ministry Of Civil Affairs, “Disaster relief tent”. [Online]. Available: https://www.gov.cn/xinwen/2016-07/28/5095541/files/50f46dff8d024193b31b6c79f3d26ecc.pdf (in Chinese).

[28] B. Yang, "Water Levels in Poyang Lake Area and the Jiujiang Section of the Yangtze River Have Reached Their Peak". [Online]. Available: https://content-static.cctvnews.cctv.com/snow-book/index.html?item_id=4327317747965904209 (in Chinese).

[29] Y. Chen, L. Duo, D. Zhao, Y. Zeng, and X. Guo, "The response of ecosystem vulnerability to climate change and human activities in the Poyang lake city group, China", *Environmental Research*, vol. 233, art. no. 116473, 2023, doi: 10.1016/j.envres.2023.116473.

[30] D. Xu, S.W. Lyon, J. Mao, H. Dai, and J. Jarsjö, "Impacts of multi-purpose reservoir construction, land-use change and climate change on runoff characteristics in the Poyang Lake basin, China", *Journal of Hydrology: Regional Studies*, vol. 29, art. no. 100694, 2020, doi: 10.1016/j.ejrh.2020.100694.

[31] D.C. Sun, H.M. Wang, J. Huang, and G.F. Liu, "Risk analysis of urban flood disaster and land type adjustment strategies in the Poyang Lake Basin: A case study of Jingdezhen City", *Resources and Environment in the Yangtze River Basin*, vol. 27, no. 12, pp. 2856–2866, 2018 (in Chinese).

[32] "Flood disaster in Jiangxi Province, 2024", Baidu Baike. [Online]. Available: https://baike.baidu.com/item/2024%E5%B9%B4%E6%B1%9F%E8%A5%BF%E6%B4%AA%E7%81%BE/64565146 (in Chinese).

[33] "Rainfall expected to continue in mid-to-late July in Jiangxi", Sina News. [Online]. Available: https://news.sina.com.cn/c/2024-07-04/doc-incaxxfi5916533.shtml (in Chinese).

[34] "Official website of the National Bureau of Statistics of China". [Online]. Available: https://www.stats.gov.cn/ [Accessed: Apr. 18, 2025] (in Chinese).

[35] Jiangxi Provincial Bureau of Statistics, "Statistical Yearbook". [Online]. Available: http://tjj.jiangxi.gov.cn/resource/nj/2023CD/zk/indexch.htm (in Chinese).

[36] Municipal Bureau of Statistics, "2022 Nanchang City Resident Population Key Data Bulletin", The People's Government of Nanchang Municipality. [Online]. Available: https://www.nc.gov.cn/ncszf/tjgb/202303 (in Chinese).

[37] L. Li, J.F. Bai, and C.P. Zhang, "Does migrant workers promote the meat consumption of rural left-behind workers", *Agricultural Technology Economics*, no. 9, pp. 27–37, 2019, doi: 10.13246/j.cnki.jae.2019.09.003 (in Chinese).

[38] B.X. Gao and W. Su, "Management of Safety Stock for Medical Emergency Supplies in Public Health Emergencies", *Journal of PLA Hospital Management*, vol. 27, no. 12, pp. 1105–1109, 2020, doi: 10.16770/J.cnki.1008-9985.2020.12.002 (in Chinese).

[39] M.X. Zhou, "Heavy rainfall in Jiangxi causes Poyang Lake and other areas to exceed warning water levels", QQ News. [Online]. Available: https://news.qq.com/rain/a/20240627A06RPN00 (in Chinese).

[40] P. Yang, Y.S. Xie, S. Ling, and Z.H. Xu, "Flood No. 1 of the Yangtze River in 2024 has formed! Latest weather warnings", 163.com. [Online]. Available: https://www.163.com/dy/article/J5PJI6950514R9OJ.html (in Chinese).

[41] H. Wu, "A study of landslide body control of black bovine cave copper ore mining and beneficiation project", *Archives of Civil Engineering*, vol. 69, no. 2, pp. 291–309, 2023, doi: 10.24425/ace.2023.145268.

Received: 2025-01-02, Revised: 2025-04-14